JACS
JOURNAL OF THE AMERICAN CHEMICAL SOCIETY

COMMUNICATION

pubs.acs.org/JACS

Hierarchical Interactions and Their Influence upon the Adsorption of Organic Molecules on a Graphene Film

Michael Roos,[‡] Daniela Künzel,[†] Benedikt Uhl,[‡] Hsin-Hui Huang,[‡] Otavio Brandao Alves,[‡] Harry E. Hoster,[‡,§] Axel Gross,[†] and R. Jürgen Behm*[,‡]

[‡]Institute of Surface Chemistry and Catalysis and [†]Institute of Theoretical Chemistry, Ulm University, D-89069 Ulm, Germany

Supporting Information

ABSTRACT: The competition between intermolecular interactions and lateral variations in the molecule−substrate interactions has been studied by scanning tunneling microscopy (STM), comparing the phase formation of (sub)-monolayers of the organic molecule 2,4′-BTP on buckled graphene/Ru(0001) and Ag(111) oriented thin films on Ru(0001). On the Ag films, the molecules form a densely packed 2D structure, while on graphene/Ru(0001), only the areas between the maxima are populated. The findings are rationalized by a high corrugation in the adsorption potential for 2,4′-BTP molecules on graphene/Ru(0001). These findings are supported by temperature programmed desorption (TPD) experiments and theoretical results.

It is well established that the formation of two-dimensional (2D) molecular networks is governed by a delicate balance between intermolecular interactions such as covalent bonds, hydrogen bonds, van der Waals interactions or, in the case of metal−organic networks, metal−ligand interactions, on the one hand, and the lateral variation in molecule−substrate interactions on the other hand.[1−10] For small lateral variations in the molecule−substrate interactions, ΔE_{ad}, as they are often observed on close-packed homogeneous surfaces such as noble metal surfaces or on highly oriented pyrolytic graphite (HOPG),[11] the resulting structures are dominated by intermolecular interactions, and the substrate−molecule interactions are mainly responsible for the preferential orientation of the respective adlayer networks.[3,4,12−15] Much less is known on the opposite case, structure formation/self-assembly of large organic molecules on homogeneous surfaces dominated by lateral variations in the molecule−substrate interactions. This case, which is highly important for the conceptual understanding of self-assembly on homogeneous surfaces and hence a key problem in surface chemistry, will be addressed in the present communication.

Here, we report on the interaction between a graphene adlayer on Ru(0001)[16] and a planar molecular adsorbate. It will be shown that this results in a situation where the energetic corrugation ΔE_{ad} is large in comparison with intermolecular interactions, which in turn results in drastic structural changes compared to adsorption on Ag(111) oriented thin films on Ru(0001), most prominently the formation of 1D molecular stripes rather than of a 2D network. The detailed understanding of the underlying physical reasons, on a molecular scale, is of fundamental importance for the understanding not only of structure formation in homogeneous surfaces with significant corrugation in the adsorption potential, but also of the adsorption behavior and structure formation of organic molecules on graphene adlayers.

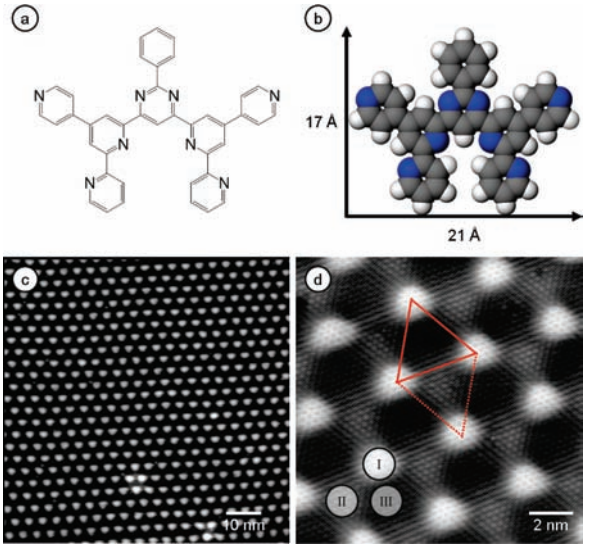

Figure 1. Schematic drawing (a) and model (b) of 2,4′-BTP with lateral dimensions; (c) large-scale STM image of a defect free area of graphene/Ru(0001) (U_T = −1.30 V, I_T = 60 pA, T = 130 K) and (d) atomically resolved STM image (U_T = 0 V, I_T = 178 pA, T = 300 K). Three different possible adsorption regions are visible: atop (I), hcp (II) and fcc (III) regions.

As molecular adsorbate, we used 2,4′-bis(terpyridine) (2,4′-BTP) (Figure 1a,b).[17,18] The numbers indicate the position of the peripheral nitrogen atoms, which are responsible for the C−H···N type hydrogen bonding between neighboring molecules. The strength of these hydrogen bonds is typically in the range of 100 meV.[18] In recent publications, we have shown that the resulting network can be tuned via the position of the outer nitrogen atoms, both at the solid/gas[14,19,20] and at the solid/liquid interface.[18,19] These previous studies were carried out on surfaces with little variation in the adsorption potential like HOPG or (111) oriented Ag thin films on Ru(0001). In the present study, a graphene monolayer supported by a Ru(0001) single crystal (graphene/Ru(0001)) is used as substrate.

Received: March 22, 2011
Published: May 23, 2011

dx.doi.org/10.1021/ja2025855 | J. Am. Chem. Soc. 2011, 133, 9208–9211

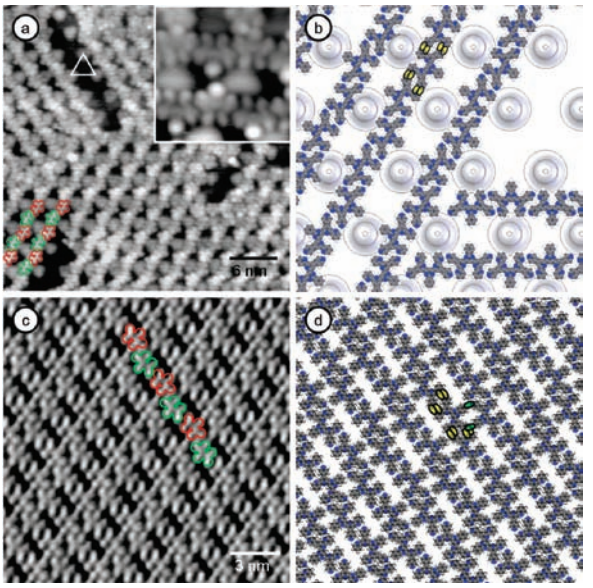

Figure 2. (a) STM image of an adlayer of 2,4′-BTP molecules on graphene/Ru(0001) (U_T = −0.97 V, I_T = 30 pA, T = 115 K). The antiparallel arrangement of the molecules is indicated by alternating colors. Inset: detail of the structure (U_T = −2.36 V, I_T = 80 pA, T = 130 K). (b) True to scale model of 2,4′-BTP admolecules on graphene with hydrogen bonding configuration (double hydrogen bonds, yellow ellipses). (c) 2,4′-BTP on Ag/Ru(0001) (U_T = −2.7 V, I_T = 5.62 pA, T = 300 K). Comparable resulting row structure, but with additional interactions between the rows. (d) Model of 2,4′-BTP on Ag/Ru(0001). Same double hydrogen bonding configuration (yellow ellipses); each molecule shares two additional single hydrogen bonds with its adjacent row (green ellipses).

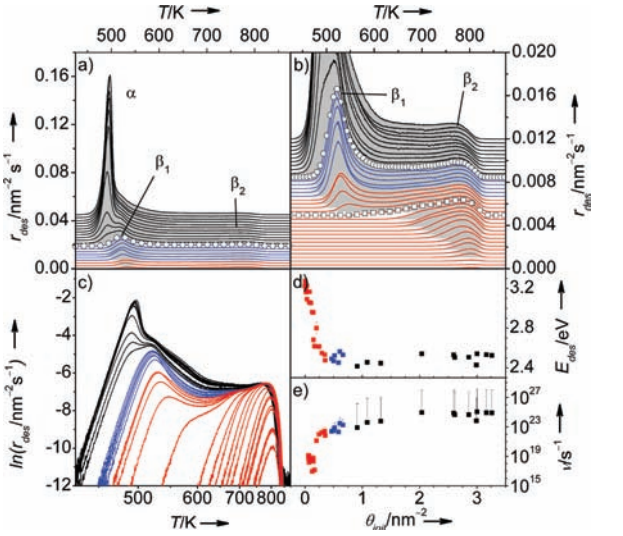

Figure 3. TPD spectra of 2,4′-BTP molecules on graphene/Ru(0001) (heating rate 1.0 K s^{-1}). Initial coverages 0.005 ≤ N_0 ≤ 3.26 nm^{-2}. (a) Overview of spectra with N_0 > 0.23 nm^{-2}. Three different adsorption states including multilayer (α-peak, black spectra), upright standing admolecules (blue spectra) and flat-lying planar adlayer (red spectra) are resolved. (b) Enlarged view of the spectra in (a), with additional low-coverage spectra. ○, N_0 = 0.66 nm^{-2}; □, N_0 = 0.21 nm^{-2}. (c) Menzel-Schlichting plot (ln(r_{des}) vs −1/T) revealing (d) E_{des} and (e) ν as function of θ_{init}.

Additional information on the energetics will be derived from thermal desorption spectroscopy and calculations.

Previous scanning tunneling microscopy (STM) measurements on graphene/Ru(0001) revealed a buckling of the graphene layer with a periodicity of 30 Å.[21] Hence, the corrugation length of the graphene layer is in the same regime as the diameter of the admolecules (∼20 Å). Figure 1c shows an exemplary image of the defect free graphene/Ru(0001) surface, while in Figure 1d, the atomic structure of the graphene layer is resolved. To guide the eye, we added a hexagonal grid. By comparison with the adsorption sites of small metal clusters on graphene/Ru(0001),[22,23] three different sites appear likely for 2,4′-BTP adsorption: the position on top of the moiré lattice (I) and the two minima marked with (II) and (III), which differ in their position with respect to the underlying Ru atoms. Recent theoretical and experimental data have shown that the observed buckling is not only an electronic effect in the STM image, but in fact reflects a real height corrugation of 1.56 Å.[24] This in turn causes lateral variations in the local electronic properties, which are decisive for the molecule−substrate interactions. In the following, we will refer to position (I) as "hill" and to (II) and (III) as "valley".

Figure 2a shows an exemplary STM image of 2,4′-BTP molecules on graphene/Ru(0001). We can clearly distinguish between the submolecularly resolved molecules and the hexagonally arranged hills of the graphene adlayer (see marked triangle). The molecules are exclusively adsorbed in the valley of the graphene while the hills remain unoccupied. This limitation to specific adsorption sites in combination with the distinct positions of the hydrogen bond donors and acceptors within the molecule results in the formation of a 1D chain structure. In that structure, two adjacent molecules are arranged in an antiparallel way (see inset in Figure 2a) To guide the eye, we marked some molecules with alternating colors in Figure 2a. The molecules in this configuration share four double hydrogen bonds (yellow ellipses in Figure 2b) with the adjacent molecules. The observation of only three different orientations of the chains, each rotated by 120° with respect to the other ones, indicates that these chains are oriented along the symmetry planes of the graphene layer. The hills act as spacers between individual chains. Because of the resulting separation of approximately 10 Å between adjacent chains, intermolecular interactions between the chains can be neglected (see inset in Figure 2a and model in Figure 2b).

Only at domain boundaries between two orientational domains, interactions between the chains are possible. The model in Figure 2b also demonstrates that the periodicity of the chains along the chain direction is not commensurate with the underlying graphene, but slightly larger. This leads to a molecular superlattice, on top of the superlattice of the graphene adlayer. The formation of molecular chains also indicates that adsorption of the molecules is not restricted to specific adsorption sites on the graphene layer as it is the case for the deposition of metal clusters on graphene.[22,25] A similar chain like structure was recently reported for the adsorption of PTCDI molecules on graphene on Rh(111).[26]

On a weakly corrugated surface such as (111) oriented thin Ag films on Ru(0001),[27] the same structural motives can be found (parallel chain structure = PCS, Figure 2c),[20] but there is no separation between the chains, in contrast to the present findings. Instead, additional intermolecular hydrogen bonds are formed between the chains (green ellipses in Figure 2d).

The fact that the hills remain unoccupied for 2,4′-BTP on graphene/Ru(0001) indicates that the corrugation of the

dx.doi.org/10.1021/ja2025855 |J. Am. Chem. Soc. 2011, 133, 9208–9211

adsorption potential exceeds the additional intermolecular interactions between the linear chains or chain elements. To get a deeper insight into the energetics of the adsorbed molecules on graphene/Ru(0001), we performed temperature programmed desorption (TPD) experiments. Desorption spectra of 2,4′-BTP molecules from graphene/Ru(0001), which are shown in Figure 3a,b (b for low coverage details), exhibit three characteristic desorption peaks. At higher coverages, a first peak appears at around 500 K (α-peak, black spectra), which we attribute to desorption from multilayer structures (3D molecular crystal). It is characterized by zero order desorption kinetics with coinciding leading edges, an upshift of the peak temperature with increasing coverage, and no saturation of the peak.

At lower initial coverage, we find an intermediate state (β_1-peak), which we associate with desorption from a densely packed layer of flat-lying, planar admolecules at coverages close to saturation of that adlayer (red spectra) and from a (partially filled) monolayer of upright molecules (blue spectra). The transition between desorption from a saturated monolayer of flat-lying molecules and molecules in an upright or tilted adsorption geometry is rather smooth, indicative of comparable interaction strengths. The same is true for the transition between the monolayer of upright molecules and the molecular crystal.

A third broad peak (β_2-peak) is attributed to desorption from a submonolayer of flat lying molecules. Evaluation of the slope and the intercept of the logarithmic desorption spectra over the reciprocal temperature (Menzel-Schlichting plot, Figure 3c)[28,29] reveals that the desorption barrier E_{des} (Figure 3d) decreases distinctly with increasing initial coverage (θ_{init}) in this coverage range. At the same time, the frequency factor ν increases strongly (Figure 3e), over several orders of magnitude from $\nu \approx 1 \times 10^{17}$ s^{-1} for low coverages until a constant value of $\nu \approx 1 \times 10^{23}$ s^{-1} is reached for higher coverages (monolayer regime). This behavior, which differs distinctly from a compensating effect,[30] also explains the width of the desorption peak. A similarly strong increase of ν at submonolayer coverages was observed and discussed in detail recently for 2,4′-BTP adsorption on HOPG.[28] It was associated with a decrease of the rotational entropy of the molecules due to a transition from freely rotating molecules at low coverages to frustrated/hindered rotation in the monolayer regime.[28] The simultaneous decrease of the activation energy for desorption, from E_{des} = 3.32 eV to E_{des} = 2.49 eV in the monolayer (and multilayer) regime can be explained by the increasing population of energetically less favorable sites within the valleys or, more likely, energetically less favorable hill sites. It is important to note that the barrier for 2,4′-BTP desorption from HOPG was found to be coverage independent.[28] Finally, E_{ad} ends in the sublimation enthalpy from a multilayer of 2,4′-BTP molecules of E_{ad} = 2.49 eV. The immediate lowering of E_{ad} with increasing coverage is also an indication that at temperatures close to desorption, hydrogen bonded networks do not exist any more. In fact, STM images recorded at temperatures as low as T = 130 K indicate the onset of mobility already at these temperatures (see Supporting Information (SI), Figure S1).

The experimental results are complemented by calculations to determine the site specific adsorption energies of 2,4′-BTP on graphene/Ru(0001). Ideally, quantum chemical calculations should be performed to evaluate the interaction energies. However, due to the size of the considered system, such calculations are prohibitively expensive. Still, for the structure of the clean graphene/Ru(0001) system, periodic density functional theory (DFT) calculations exist for a 12 × 12 graphene layer on a 11 × 11 Ru(0001)

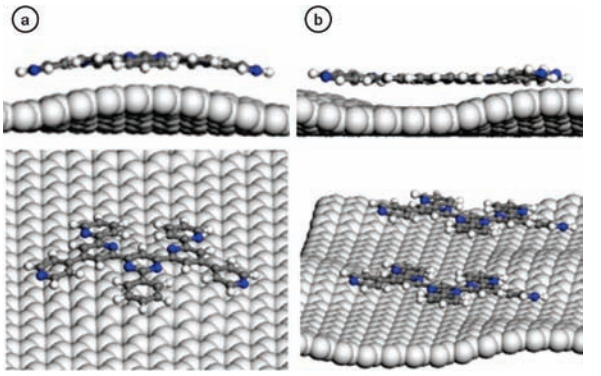

Figure 4. Side and perspective view of the simulated adsorption geometry of a single 2,4′-BTP molecule on a hill (a) and valley (b) position.

slab with three layers (lattice constant 29.96 Å).[16] We used the structure of the graphene/Ru(0001) slab resulting from these calculations, and determined the 2,4′-BTP adsorption energies on that substrate using the COMPASS force-field[31] which has been shown to give an acceptable representation of the BTP/graphite system,[32] for the BTP-graphene interaction, together with an additional dispersion term to account for the long-range BTP-Ru interaction. Metals and molecule-metal interaction are typically not properly reproduced within force fields calculations. To obtain a reliable description of the long-range interaction between the BTP-molecule and the Ru(0001) substrate which are separated by at least 5 Å, we employed a semiempirical dispersion correction scheme,[33,34] which is normally used to include van der Waals interaction in standard DFT methods.[35]

In the calculations, the graphene/Ru system was kept fixed, while the BTP molecular structure was allowed to relax for the two different adsorption sites ("hill" and "valley"). The different adsorption sites lead to a distortion of the molecules as illustrated in Figure 4a for a "hill" and in Figure 4b for a "valley" position. The difference of the adsorption energies on a "hill" (E_{hill} = −3.45 eV) and a "valley" (E_{valley} = −4.08 eV) position results in a substantial corrugation of the adsorption energy of ΔE = 0.63 eV. Not only the van der Waals interactions between the 2,4′-BTP molecules and the underlying Ru substrate contribute to the overall interactions and the corrugation, but there is also a non-negligible contribution from the interactions with the graphene (see SI).

In passing, we note that we also used other force fields to calculate the 2,4′-BTP adsorption energies, and all of them gave rather similar values for the corrugation (see the Supporting Information, where also the BTP interactions with the single Ru layers are listed). The corrugation is substantial compared to the intermolecular interaction. If the rows of molecules were much closer (like on a Ag thin film on Ru(0001)), they would form a 2D network and gain an additional binding energy of 0.100 eV per molecule from H-bridge bonds,[18] which is significantly less than the energetic corrugation for 2,4′-BTP on graphene/Ru(0001). Note also that the total intermolecular interaction energies for BTP in a two-dimensional hexagonal structure on graphite only amounts to about 0.4 eV,[32] which is also less than the energetic corrugation listed above.

In total, we could show by a combination of structural (STM) and energetic (TPD, theoretical calculations) information that the formation of 1D intermolecular chain structures on a substrate

dx.doi.org/10.1021/ja2025855 |J. Am. Chem. Soc. 2011, 133, 9208–9211

with a highly corrugated adsorption potential (graphene/Ru(0001)) can be quantitatively explained by the concept based on the competition between intermolecular interactions of 'normal' strength and a pronounced lateral variation of the molecule—substrate interactions. Hence, our findings demonstrate that this concept is also applicable in the structure formation on homogeneous surfaces with high lateral variation of the adsorption potential, confirming the validity of this concept for the description of self-assembly processes of large organic molecules on homogeneous surfaces in general. Furthermore, it emphasizes the important role of supported graphene as a new substrate in surface chemistry.

■ ASSOCIATED CONTENT

Supporting Information. Experimental and theoretical details, tables with results of calculations. This material is available free of charge via the Internet at http://pubs.acs.org.

■ AUTHOR INFORMATION

Corresponding Author
juergen.behm@uni-ulm.de

Present Addresses
[§]TUM CREATE Centre for Electromobility, 62 Nanyang Drive, Singapore.

■ ACKNOWLEDGMENT

We thank Marie-Laure Bocquet and Ulrich Ziener for providing the coordinates of the graphene layer and the BTP material, respectively. The work was supported by the Deutsche Forschungsgemeinschaft via the Collaborative Research Centre (SFB) 569.

■ REFERENCES

(1) Elemans, J. A. A. W.; Lei, S.; De Feyter, S. *Angew. Chem., Int. Ed.* **2009**, *48*, 7298.
(2) Barth, J. V.; Constantini, G.; Kern, K. *Nature* **2005**, *437*, 671.
(3) Barth, J. V. *Annu. Rev. Phys. Chem.* **2007**, *58*, 375.
(4) Bartels, L. *Nat. Chem.* **2010**, *2*, 87.
(5) Cheng, D.; Wang, W.; Huang, S. *J. Phys. Chem. C* **2007**, *111*, 1631.
(6) Cicoira, F.; Miwa, J. A.; Perepichka, D. F.; Rosei, F. *J. Phys. Chem. A* **2007**, *111*, 12674.
(7) Barrena, E.; Palacios-Lidón, E.; Munuera, C.; Torrelles, X.; Ferrer, S.; Jonas, U.; Salmeron, M.; Ocal, C. *J. Am. Chem. Soc.* **2004**, *126*, 385.
(8) Oteyza, D. G. d.; Silanes, I.; Ruiz-Osés, M.; Barrena, E.; Doyle, B. P.; Arnau, A.; Dosch, H.; Wakayama, Y.; Ortega, J. E. *Adv. Funct. Mat.* **2009**, *19*, 259.
(9) Schnadt, J.; Xu, W.; Vang, R. T.; Knudsen, J.; Li, Z.; Laegsgaard, E.; Besenbacher, F. *Nano. Res.* **2010**, *3*, 459.
(10) Lu, B.; Iimori, T.; Sakamoto, K.; Nakatsuji, K.; Rosei, F.; Komori, F. *J. Phys. Chem. C* **2009**, *112*, 10187.
(11) Forrest, S. R. *Chem. Rev.* **1997**, *97*, 1793.
(12) Klappenberger, F.; Canas-Ventura, M. E.; Clair, S.; Pons, S.; Schlikum, U.; Qu, Z.-R.; Strunskus, T.; Comisso, A.; Wöll, C.; Brune, H.; De Vita, A.; Ruben, M.; Barth, J. V. *Chem. Phys. Chem.* **2008**, *9*, 2522.
(13) Hermann, B. A.; Rohr, C.; Balbás Gambra, M.; Maleki, A.; Malarek, M. S.; Frey, E.; Franosch, T. *Phys. Rev. B* **2010**, *82*, 165451.
(14) Hoster, H. E.; Roos, M.; Breitruck, A.; Meier, C.; Tonigold, K.; Waldmann, T.; Ziener, U.; Behm, R. J. *Langmuir* **2007**, *23*, 11570.
(15) Waldmann, T.; Reichelt, R.; Hoster, H. *Chem. Phys. Chem.* **2010**, *11*, 1513.
(16) Wang, B.; Bocquet, M.-L.; Marchini, S.; Günther, S.; Wintterlin, J. *Phys. Chem. Chem. Phys.* **2008**, *10*, 3530.
(17) Ziener, U.; Lehn, J. M.; Mourran, A.; Möller, M. *Chem.—Eur. J.* **2002**, *8*, 951.
(18) Meier, C.; Ziener, U.; Landfester, K.; Weihrich, P. *J. Phys. Chem. B* **2005**, *109*, 21015.
(19) Meier, C.; Roos, M.; Künzel, D.; Breitruck, A.; Hoster, H. E.; Landfester, K.; Gross, A.; Behm, R. J.; Ziener, U. *J. Phys. Chem. C* **2010**, *114*, 1268.
(20) Roos, M.; Hoster, H. E.; Breitruck, A.; Behm, R. J. *Phys. Chem. Chem. Phys.* **2007**, *9*, 5672.
(21) Marchini, S.; Günther, S.; Wintterlin, J. *Phys. Rev. B* **2007**, *76*, 075429.
(22) Donner, K.; Jakob, P. *J. Chem. Phys.* **2009**, *131*, 164701.
(23) Zhou, Z.; Gao, F.; Goodman, D. W. *Surf. Sci.* **2010**, *604*, 31.
(24) Moritz, W.; Wang, B.; Bocquet, M.-L.; Brugger, T.; Greber, T.; Wintterlin, J.; Günther, S. *Phys. Rev. Lett.* **2010**, *104*, 136102.
(25) Zhou, Y.; Zhou, J. *J. Phys. Chem. Lett.* **2010**, *1*, 609.
(26) Pollard, A. J.; et al. *Angew. Chem., Int. Ed.* **2010**, *49*, 1794.
(27) Ling, W. L.; de la Figuera, J.; Bartelt, N. C.; Hwang, R. Q.; Schmid, A. K.; Thayer, G. E.; Hamilton, J. C. *Phys. Rev. Lett.* **2004**, *92*, 116102.
(28) Roos, M.; Breitruck, A.; Hoster, H. E.; Behm, R. J. *Phys. Chem. Chem. Phys.* **2010**, *12*, 818.
(29) Schlichting, H.; Menzel, D. *Surf. Sci.* **1992**, *272*, 27.
(30) Niemantsverdiet, J. W.; Wandelt, K. *J. Vac. Sci. Technol., A* **2011**, *6*, 757.
(31) Sun, H. *J. Phys. Chem. B* **1998**, *102*, 7338.
(32) Künzel, D.; Markert, Th.; Gross, A.; Benoit, D. *Phys. Chem. Chem. Phys.* **2009**, *11*, 8867.
(33) Grimme, S. *J. Comput. Chem.* **2006**, *27*, 1787.
(34) Grimme, S.; Antony, J.; Ehrlich, S.; Krieg, H. *J. Chem. Phys.* **2010**, *132*, 154104.
(35) Tonigold, K.; Gross, A. *J. Chem. Phys.* **2010**, *132*, 224701.